

Magnetic blocking in a linear iron(II) complex

Joseph M. Zadrozny¹, Dianne J. Xiao¹, Mihail Atanasov^{2,3}, Gary J. Long⁴, Fernande Grandjean⁴, Frank Neese³ and Jeffrey R. Long^{1*}

Single-molecule magnets that contain one spin centre may represent the smallest possible unit for spin-based computational devices. Such applications, however, require the realization of molecules with a substantial energy barrier for spin inversion, achieved through a large axial magnetic anisotropy. Recently, significant progress has been made in this regard by using lanthanide centres such as terbium(III) and dysprosium(III), whose anisotropy can lead to extremely high relaxation barriers. We contend that similar effects should be achievable with transition metals by maintaining a low coordination number to restrict the magnitude of the *d*-orbital ligand-field splitting energy (which tends to hinder the development of large anisotropies). Herein we report the first two-coordinate complex of iron(II), [Fe(C(SiMe₃)₂)₂]⁻, for which alternating current magnetic susceptibility measurements reveal slow magnetic relaxation below 29 K in a zero applied direct-current field. This $S = \frac{3}{2}$ complex exhibits an effective spin-reversal barrier of $U_{\text{eff}} = 226(4) \text{ cm}^{-1}$, the largest yet observed for a single-molecule magnet based on a transition metal, and displays magnetic blocking below 4.5 K.

Nearly a decade ago it was discovered that the mononuclear lanthanide complexes [LnPc]⁻ (H₂Pc = phthalocyanine; Ln = Tb, Dy) possessed directionally bistable magnetic moments¹. In these molecules, the spin and orbital angular momenta couple strongly to generate inherent directionality for the molecular magnetic moments. As a result of these highly anisotropic spin-orbit coupled ground states and the relaxation barriers imposed by the axial ligand fields², the magnetic moments of these molecules reorient only slowly on removal from a magnetizing field. When the relaxation time is sufficiently long, molecular magnetic hysteresis is observed, similar to that of classical magnets, but here owing to the moment of a single metal ion³. Significantly, the effective relaxation barriers for such species, determined by spectral and/or magnetic susceptibility measurements, can be as high as $U_{\text{eff}} = 641 \text{ cm}^{-1}$ (refs 2–6), which surpasses by an order of magnitude that obtained for the original single-molecule magnet, Mn₁₂O₁₂(O₂CCH₃)₁₆(H₂O)₄ (refs 7,8) and other clusters that contain transition metals^{9,10}. Thus, *f*-element complexes appear to present the best opportunities for attaining the high relaxation barriers required for potential applications of single-molecule magnets in information storage¹¹, quantum computation^{11–14} and spintronics¹⁵.

The investigation of the magnetic anisotropies of systems based on transition metals is of renewed interest as part of a larger general effort to find magnetic alternatives to the *f*-block elements. However, compared to lanthanides and actinides, mononuclear complexes of transition metals appear to be poorly suited to achieving high relaxation barriers because of their smaller magnetic moments and, at least for first-row transition-metal ions, lower spin-orbit coupling (SOC) constants. In addition, the larger ligand-field splitting energies of the transition-metal *d* orbitals can be expected to suppress the orbital contributions to the magnetism required to develop magnetic anisotropy. In one manifestation of this effect, first-order orbital angular momentum can be quenched as the result of a Jahn–Teller distortion¹⁶. In another, the second-order contribution to the magnetic anisotropy (that is, zero-field splitting) is diminished because of the large energy separation

between ground and excited electronic states, which reduces the degree of mixing. Importantly, these ligand-field effects can be overcome substantially by enforcing a low coordination number at the transition-metal centre, which causes the *d* orbitals to fall within a narrow energy range, similar to the situation found for the 4*f* orbitals of a lanthanide complex. Indeed, four-coordinate trigonal pyramidal complexes of iron(II) with an $S = 2$ ground state were shown to behave as single-molecule magnets with thermal relaxation barriers as high as 65 cm^{-1} (refs 17,18). In these and a number of other mononuclear transition-metal complexes^{19–22}, however, the observation of slow magnetic relaxation requires a d.c. field bias to suppress fast magnetization reversal through quantum tunnelling. Alternatively, tunnelling of the magnetic moment caused by mixing of the ground $\pm M_S$ levels will be minimized in half-integer spin systems, as posited by Kramers²³. Thus, such systems should not require a d.c. field bias to display slow magnetic relaxation. As initial examples, recently the $S = \frac{3}{2}$ complexes in (Ph₄P)₂[Co(SPh)₄] and (PNP)FeCl₂ (PNP⁻ = N[2-P(CHMe₂)₂-4-methylphenyl]₂ anion) were shown to behave as single-molecule magnets in the absence of an applied d.c. field, exhibiting $U_{\text{eff}} = 21(1)$ and $34(2) \text{ cm}^{-1}$, respectively^{24,25}.

A linear two-coordinate geometry presents perhaps the best opportunity for mitigating ligand-field effects in transition-metal complexes and creating a large anisotropy barrier²⁶. Here, a high-spin *d*⁶-electron configuration can be expected to provide unquenched orbital angular momentum, which maximizes the magnitude of the magnetic moment and the ligands define an axis for its preferential alignment. Recently, we and others studied linear, two-coordinate complexes of iron(II), which possess $S = 2$ ground states under the influence of an unquenched orbital angular momentum^{27–31}. These investigations revealed that very large spin-reversal barriers, as high as 181 cm^{-1} , could be observed by a.c. magnetic susceptibility measurements, albeit only in the presence of an applied d.c. field. To determine if such large barriers could be attained in the absence of an applied field, again taking advantage of Kramers' theorem, we chose to investigate the magnetic properties of two-coordinate complexes with $S = \frac{3}{2}$ ground

¹Department of Chemistry, University of California, Berkeley, California 94720-1460, USA, ²Max-Planck Institut für Chemische Energiekonversion, Mülheim an der Ruhr, D-45470, Germany, ³Institute of General and Inorganic Chemistry, Bulgarian Academy of Sciences, Academy Georgi Bontchev, Sofia, 1113 Bulgaria, ⁴Department of Chemistry, University of Missouri-Rolla, Rolla, Missouri 65409-0010, USA. *e-mail: jrlong@berkeley.edu

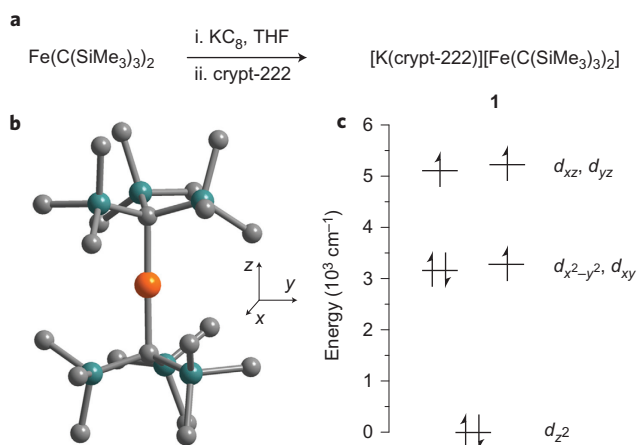


Figure 1 | Preparation, structure and *d*-orbital splitting of the linear iron(I) complex $[\text{Fe}(\text{C}(\text{SiMe}_3)_3)_2]^-$. **a**, General reaction scheme for the synthesis of **1**. **b**, Structure of the $[\text{Fe}(\text{C}(\text{SiMe}_3)_3)_2]^-$ anion, as observed in the crystal structure of **1**. Orange, cyan and grey spheres represent Fe, Si and C, respectively; H atoms are omitted for clarity. Selected interatomic distances (Å) and angles ($^\circ$) for **1**: Fe–C = 2.062(4), 2.058(4), Fe...Fe = 9.211(3); C–Fe–C = 179.2(2). **c**, Energies of the 3*d* orbitals extracted from an *ab initio* computational analysis of $[\text{Fe}(\text{C}(\text{SiMe}_3)_3)_2]^-$.

states. Here we report the first two-coordinate complex of iron(I), $[\text{Fe}(\text{C}(\text{SiMe}_3)_3)_2]^-$, that, indeed, possesses a highly anisotropic $S = \frac{3}{2}$ spin state and gives a record high barrier for magnetic relaxation in a transition-metal complex under a zero applied field.

Results and discussion

The viability of reducing the linear two-coordinate complex $\text{Fe}(\text{C}(\text{SiMe}_3)_3)_2$ by one electron was first recognized on measuring its cyclic voltammogram in difluorobenzene (Supplementary Fig. S1). Here, a reversible reduction event that corresponded to the $[\text{Fe}(\text{C}(\text{SiMe}_3)_3)_2]^{0/1-}$ couple is apparent at $E_{1/2} = -1.82$ V versus the $[\text{FeCp}_2]^{1+/0}$ ($\text{Cp}^- = \text{cyclopentadienyl anion}$) couple with a peak-to-peak separation of 78 mV. In view of this result, KC_8 was employed to reduce the complex, which, on addition of 2.2.2-cryptand (crypt-222), enabled isolation of the yellow-green compound $[\text{K}(\text{crypt-222})][\text{Fe}(\text{C}(\text{SiMe}_3)_3)_2]$ (**1**). X-ray diffraction analysis of a single crystal of **1** revealed the linear two-coordinate structure of $[\text{Fe}(\text{C}(\text{SiMe}_3)_3)_2]^-$, as depicted in Fig. 1 (see also Supplementary Fig. S2). Here, the C–Fe–C angle of $179.2(2)^\circ$ is almost perfectly linear, which places **1** among a small family of homoleptic two-coordinate metal(I) complexes of the $[\text{C}(\text{SiMe}_3)_3]^-$ ligand^{32–35}. Notably, the SiMe_3 groups are nearly eclipsed, in contrast to the structure of $\text{Fe}(\text{C}(\text{SiMe}_3)_3)_2$ in which they are staggered³⁶. The Fe–C distances of 2.058(4) and 2.062(4) Å are only marginally longer than the distance of 2.051(1) Å in $\text{Fe}(\text{C}(\text{SiMe}_3)_3)_2$ (ref. 36).

Compound **1** was characterized by ^{57}Fe Mössbauer spectroscopy, a technique that is highly sensitive to the oxidation state and chemical environment of the iron centre. Although the structures of the linear complexes in $\text{Fe}(\text{C}(\text{SiMe}_3)_3)_2$ and **1** are very similar, different Mössbauer parameters are observed for the two compounds, in agreement with a change in the oxidation state of the iron on reaction with KC_8 . The spectrum of $\text{Fe}(\text{C}(\text{SiMe}_3)_3)_2$ at 295 K consists of a quadrupole doublet broadened by paramagnetic relaxation and characterized by an isomer shift of $\delta = 0.39(1) \text{ mm s}^{-1}$, a quadrupole splitting of $\Delta E_Q = -1.08(1) \text{ mm s}^{-1}$ and an internal hyperfine field of $H_{\text{int}} = 152 \text{ T}$ (Supplementary Fig. S3)²⁷. For **1**, an asymmetric quadrupole doublet is also observed at 295 K (Fig. 2), which indicates the onset of slow paramagnetic relaxation on the Mössbauer timescale. At 5 K, the spectrum has a sharp sextet,

and a fit yields $H_{\text{int}} = 63.97(1) \text{ T}$. To account for the paramagnetic relaxation, the 295 K spectrum was fit with a relaxation profile with $H_{\text{int}} = 63.97(1) \text{ T}$, which yielded $\delta = 0.278(4) \text{ mm s}^{-1}$, $\Delta E_Q = -2.520(7) \text{ mm s}^{-1}$ and a magnetic relaxation time $\tau = 5.1(6) \times 10^{-11} \text{ s}$. These parameters are consistent with a change in oxidation state for the two-coordinate iron(I) ion and furthermore mirror similar trends observed in three-coordinate^{37,38} and four-coordinate³⁹ iron(II/I) systems.

A ligand-field analysis of the results of *ab initio* calculations performed on **1** based on the methods described previously³¹ provided the *d*-orbital splitting depicted in Fig. 1c (see also Supplementary Information). The calculations demonstrate that the combination of a low coordination number and a low oxidation state generates a very weak ligand field. This situation has important consequences for the electronic structure and magnetic properties of **1**: (1) a very strong $4s-3d_{z^2}$ mixing is induced and (2) an almost unquenched orbital momentum arises. Together, these two features are probably the origin of the relatively low δ and large H_{int} observed in the Mössbauer spectra. SOC leads to a splitting of the ^4E ground state of **1** into four doublets that are best characterized by the quantum number M_J , where J refers to the total angular momentum of the system. In order of increasing energy, these doublets correspond to the quantum numbers $M_J = \pm\frac{7}{2}, \pm\frac{5}{2}, \pm\frac{3}{2}$ and $\pm\frac{1}{2}$ (Supplementary Table S3). The energy spacings between these doublets are approximately $\frac{2}{3}\zeta$, where ζ is the effective SOC constant ($\zeta = 361 \text{ cm}^{-1}$ for a free iron(I) ion).

The variable-temperature d.c. magnetic susceptibility data for **1** collected under a 1 kOe applied d.c. field reveal non-Curie law behaviour, consistent with a highly anisotropic magnetic moment (Fig. 3). At 300 K, $\chi_M T = 3.39 \text{ cm}^3 \text{ K mol}^{-1}$, lower than the $4.80 \text{ cm}^3 \text{ K mol}^{-1}$ observed for $\text{Fe}(\text{C}(\text{SiMe}_3)_3)_2$, yet significantly higher than the value of $1.875 \text{ cm}^3 \text{ K mol}^{-1}$ expected for an

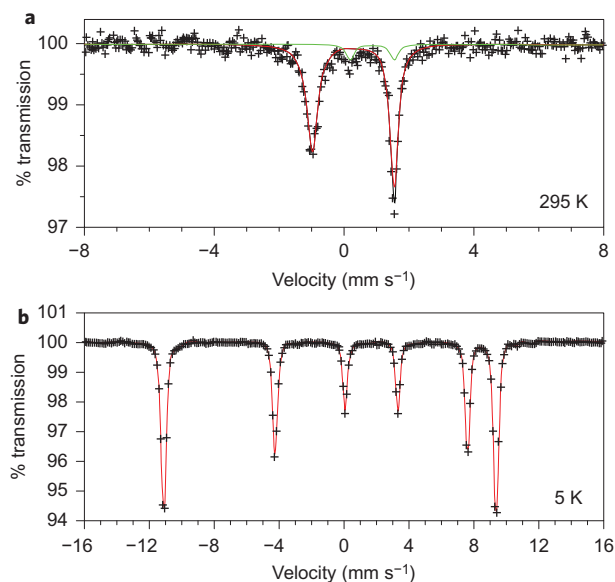


Figure 2 | Mössbauer spectra for crystalline **1** measured at 295 and 5 K.

a, Data collected at 295 K. The black line (mostly overlaid by the red line and data points) represents the sum of two fitted components. The major component, red, corresponds to **1** and the second component, green, corresponds to a minor unidentified, oxidized impurity. The red component is a result of a fit with a relaxation profile calculated for a fixed experimental linewidth of 0.314 mm s^{-1} and with $\delta = 0.278(4) \text{ mm s}^{-1}$, $\Delta E_Q = -2.520(7) \text{ mm s}^{-1}$, $H_{\text{int}} = 63.97(1) \text{ T}$, $\tau = 5.1(6) \times 10^{-11} \text{ s}$ and 90.0(5) % area. **b**, Data collected at 5 K. The red line corresponds to a fit with $\delta = 0.410(2) \text{ mm s}^{-1}$, $\Delta E_Q = -2.557(5) \text{ mm s}^{-1}$, $H_{\text{int}} = 63.97(1) \text{ T}$ and $\Gamma = 0.314(2) \text{ mm s}^{-1}$.

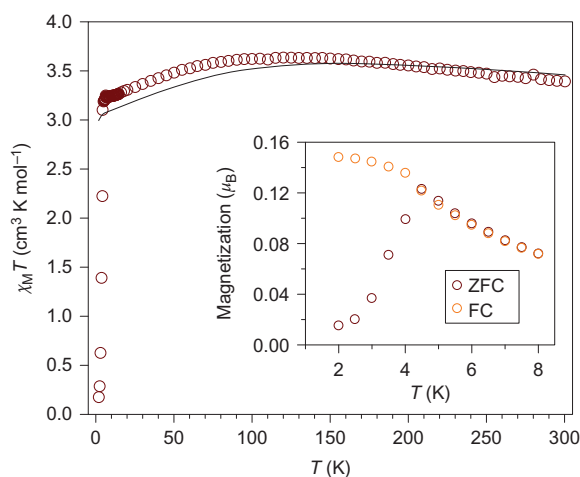


Figure 3 | Variable-temperature molar magnetic susceptibility and field-cooled versus zero-field cooled magnetization data. Data for a microcrystalline sample of **1** were collected under a 1 kOe applied d.c. field at temperatures from 2 to 300 K. The black line corresponds to a simulated set of susceptibility data that utilizes the electronic structure determined computationally, as described in the main text. The inset shows low-temperature magnetization data that highlight a divergence at 4.5 K, indicative of magnetic blocking that arises when the sample is cooled under a 1 kOe applied d.c. field (FC) compared to cooling under a zero d.c. field (ZFC).

isotropic $S = \frac{3}{2}$ metal centre. As the temperature is lowered, $\chi_M T$ increases to a maximum of $3.64 \text{ cm}^3 \text{ K mol}^{-1}$ at 125 K and then gradually decreases to $3.21 \text{ cm}^3 \text{ K mol}^{-1}$ at 5.5 K before it drops precipitously to $0.18 \text{ cm}^3 \text{ K mol}^{-1}$ at 2 K. The $\chi_M T$ data above 5.5 K are typical for transition-metal complexes with first-order orbital angular momenta. Further, there is close agreement between the experimental data and the simulations on the basis of the electronic structure results (Fig. 3 and Supplementary Fig. S4)^{30,31}.

The large energy splittings of the M_J sublevels obtained from the *ab initio* calculations indicate that $[\text{Fe}(\text{C}(\text{SiMe}_3)_2)_2]^-$ should behave as a single-molecule magnet with a substantial energy barrier. As a direct probe of the relaxation dynamics, a.c. magnetic susceptibility measurements were performed on a microcrystalline sample of **1**. Variable-frequency, variable-temperature in-phase (χ'_M) and out-of-phase (χ''_M) a.c. magnetic susceptibility data were collected under a 4 Oe a.c. field at frequencies (ν) of 0.1 to 1,488 Hz from 9 to 29 K at a zero applied d.c. field. As shown in Fig. 4, the maximum in the χ''_M versus ν plot shifts to higher frequencies with increasing temperature until it moves beyond the high-frequency limit of the instrument at 29 K. At a given temperature, the ν at which a maximum occurs in χ''_M corresponds to $\nu = (2\pi\tau)^{-1}$. Thermally activated spin-reversal⁴⁰ yields an exponential dependence of τ on temperature: $\tau = \tau_0 \exp(U_{\text{eff}}/k_B T)$, where τ_0 is the attempt time, U_{eff} is the effective spin-reversal barrier and k_B is the Boltzmann constant. The resulting Arrhenius plot for **1** reveals a linear set of data from 20 to 29 K, which indicates dominant spin relaxation through an Orbach mechanism (see Fig. 4). A linear fit to this regime yields $U_{\text{eff}} = 226(4) \text{ cm}^{-1}$ (325(6) K) and $\tau_0 = 1.3(3) \times 10^{-9} \text{ s}$. The former value is the largest relaxation barrier yet reported for single-molecule magnets that contain either one (181 cm^{-1})³⁰ or multiple transition-metal centres (67 cm^{-1})¹⁰, although τ_0 is within the range of 10^{-7} to 10^{-10} s expected for a molecular species³. The value of U_{eff} is close to the calculated energy gap of 210 cm^{-1} between the ground $M_J = \frac{7}{2}$ pair and the first excited doublet $M_J = \frac{5}{2}$, which suggests that the magnetic relaxation proceeds via this latter state. Below 20 K, τ deviates

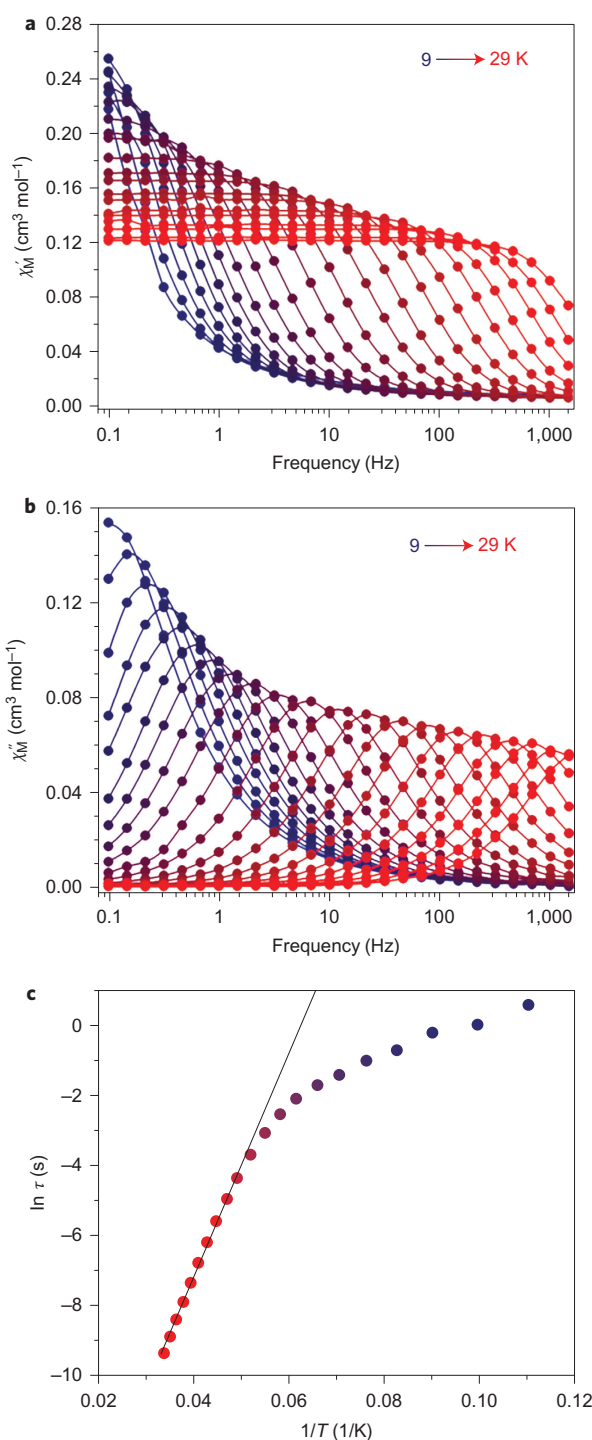


Figure 4 | Dynamic magnetic data for 1. **a, b**, Variable-temperature, variable-frequency in-phase (χ'_M) (**a**) and out-of-phase (χ''_M) (**b**) components of the a.c. magnetic susceptibility data collected for **1** under a zero applied d.c. field from 9 to 29 K. For a given temperature, a peak in χ''_M indicates an energy barrier with respect to spin reversal. **c**, Arrhenius plot of the natural log of the relaxation time, τ , versus the inverse temperature. Standard deviations of the relaxation times were determined from a nonlinear least-squares analysis using the program SolverAid (Version 7) by R. de Levie (Microsoft Excel Macro, 2007)); error bars are omitted as they are within the radius of the symbols. The black line corresponds to a fit of the data in the range 20–29 K to the Arrhenius expression $\tau = \tau_0 \exp(U_{\text{eff}}/k_B T)$, which affords $U_{\text{eff}} = 226(4) \text{ cm}^{-1}$ (325(6) K) and $\tau_0 = 1.3(3) \times 10^{-9} \text{ s}$ with $R^2 = 0.997$.

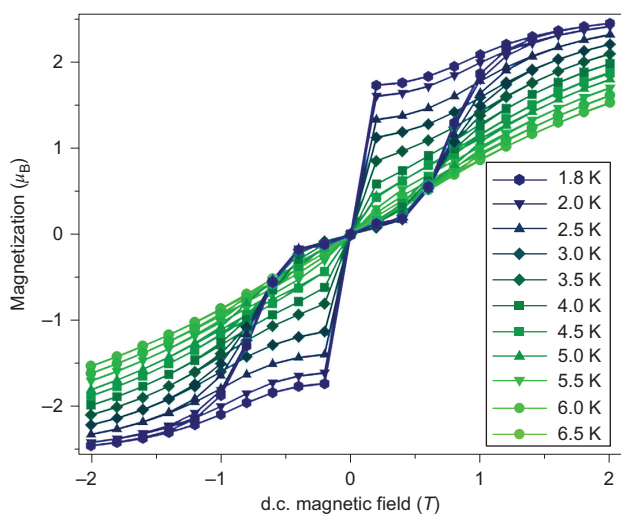


Figure 5 | Variable-field magnetization data for 1. Data were collected at an average sweep rate of 50 Oe s^{-1} by starting at $H = 0 \text{ T}$, sweeping to $H = +2 \text{ T}$ and then cycling to -2 T and back to $+2 \text{ T}$. Data were obtained at 1.8 K first, and then collected with increasing temperature. Solid lines are guides for the eye. As the magnetic field is swept from 2 to -2 T and back, hysteretic behaviour is clearly observed for $H_{dc} \neq 0$, which indicates slow magnetic relaxation with relaxation times on the order of minutes for these fields. Waist-restricted magnetic hysteresis loops are observed for all data from 1.8 to 6.5 K and result from rapid tunnelling once a measurement is taken at 0 T .

from an exponential temperature dependence, indicating the emergence of tunnelling relaxation processes that short cut the energy barrier.

A nearly discontinuous decrease in $\chi_M T$ at low temperature, as apparent in Fig. 3, can signify the blocking of the magnetic moments by a spin-reversal barrier. In such a case, a difference will be apparent in magnetic susceptibility data collected on cooling the sample with or without an applied d.c. field. Indeed, such a difference is observed for **1** below 4.5 K (see inset to Fig 3), which indicates that the magnetic moments of **1** at these low temperatures are blocked from reorientation on application of a 1 kOe d.c. field . This result further suggests that magnetic hysteresis should be apparent at these temperatures. Consistently, hysteresis is observed for $H \neq 0 \text{ Oe}$, as demonstrated for a microcrystalline sample of **1** by variable-field magnetization data collected from 1.8 to 6.5 K under applied fields of up to 2 T (Fig. 5). At zero field, however, the hysteresis loops collected at an average sweep rate of 50 Oe s^{-1} suddenly close to give a waist-restricted shape. This feature results from the presence of tunnelling pathways for the magnetic relaxation, which, as indicated by the relaxation times obtained from the a.c. susceptibility data (Fig. 4), can occur at zero field on a timescale faster than the magnetic measurement.

Among several possibilities⁴¹, intermolecular dipolar interactions have been implicated as facilitating tunnelling in mononuclear transition metal²⁴, lanthanide^{5,42,43} and actinide^{43,44} single-molecule magnets. To probe this possibility, magnetic measurements were performed on frozen solutions of **1** in 2-methyltetrahydrofuran. The resulting a.c. magnetic susceptibility data reveal slowly relaxing magnetic moments completely analogous to the data obtained for microcrystalline samples (Supplementary Fig. S6), which offers proof of the molecular nature of the slow magnetization dynamics. Indeed, above 8 K the temperature dependence of τ indicates a relaxation barrier for $[\text{Fe}(\text{C}(\text{SiMe}_3)_3)_2]^-$ in frozen solution that is identical to that observed in the crystals. For a 4 mM solution of **1**—the lowest concentration for which reliable data could be

obtained—the relaxation times at low temperature are, indeed, somewhat slower than those in the crystals, by as much as a factor of two at 10 K . There is, however, still a significant deviation from strict Arrhenius behaviour at these low temperatures, which indicates that dipolar interactions are not the sole facilitators of tunnelling. Geometric distortions in solution could also be a factor, as deviations from strict axial symmetry can induce mixing of the ground $M_J = \pm \frac{7}{2}$ levels and enable tunnelling. To a lesser extent, such an effect may also be operative in the crystalline phase given the slight deviation from linearity associated with the apparent C–Fe–C angle of $179.2(2)^\circ$ and possible Renner–Teller vibronic activity reflected by the anisotropic thermal ellipsoids of the iron(i) ion. Magnetization data collected on the frozen solutions of **1** display waist-restricted hysteresis loops similar to those collected for the crystalline phase (Supplementary Fig. S7). In this case, however, the loops remained slightly open at zero field, presumably because of the increased relaxation times observed on elimination of dipolar effects.

Outlook

As exemplified with the linear iron(i) complex $[\text{Fe}(\text{C}(\text{SiMe}_3)_3)_2]^-$ ($U_{\text{eff}} = 226 \text{ cm}^{-1}$), the foregoing results demonstrate that a two-coordinate transition-metal complex with an odd electron count can behave as a single-molecule magnet with an extremely high spin-reversal barrier in a zero applied field. Importantly, the axial ligand field imposed at the transition-metal centre directs the ion towards a large magnetic anisotropy, which leads to relaxation properties akin to those observed for lanthanide complexes, and suggests that low-coordinate transition-metal centres could potentially serve as replacements for lanthanides in hard permanent magnets. Future efforts will explore the effects of modifying the ligand field in related linear $S = \frac{3}{2}$ complexes, with particular emphasis on further enhancing magnetic anisotropy by bringing the d_{z^2} orbital lower in energy and ensuring minimal quenching of the orbital angular momentum. In addition, we will investigate the possibility of mitigating tunnelling pathways by engaging such metal centres in strong magnetic exchange interactions that create higher spin ground states, as recently demonstrated for lanthanide systems^{45,46}.

Methods

A solution of $\text{Fe}(\text{C}(\text{SiMe}_3)_3)_2$ (0.10 g , 0.19 mmol) in 2 ml of tetrahydrofuran (THF) was added to a slurry of KC_8 (26 mg , 0.19 mmol) in 2 ml of THF. On stirring vigorously for two hours, the solution changed from a deep-red to a bright yellow-orange colour. The solution was filtered through diatomaceous earth (Celite 545), and crypt-222 (74 mg , 0.20 mmol) was added. The solvent was removed under reduced pressure to afford a crude product, which was washed with 10 ml of hexanes to remove unreacted $\text{Fe}(\text{C}(\text{SiMe}_3)_3)_2$, dried under nitrogen flow and dissolved in 100 ml of $^i\text{Pr}_2\text{O}$. Hexanes were layered on top of the solution, which led to the formation of bright yellow-green block-shaped crystals of **1** (65 mg , 49%). Electrospray ionization mass spectroscopy (ESI/MS) (m/z): calculated for $[\text{Fe}(\text{C}(\text{SiMe}_3)_3)_2]^-$, 518.219 ; found, 518.217 . Ultraviolet-visible spectroscopy (2-MeTHF): λ_{max} (nm) (ϵ_M ($\text{M}^{-1} \text{ cm}^{-1}$)) 845 ($1,456$), 723 ($3,270$), 596 ($1,023$), 417 ($7,040$). Infrared (Nujol) (cm^{-1}): $2,942$ (m), $2,922$ (w), $2,885$ (m), $2,814$ (w), $1,477$ (m), $1,459$ (m), $1,445$ (m), $1,354$ (s), $1,296$ (s), $1,259$ (w), $1,241$ (vs), $1,230$ (w), $1,174$ (w), $1,133$ (s), $1,103$ (vs), $1,078$ (s), $1,058$ (w), $1,029$ (w), 950 (s), 932 (s), 865 (vs), 824 (vs), 770 (s), 754 (m), 665 (s), 644 (vs), 606 (s), 591 (s), 566 (w), 523 (m). Analytically calculated for $\text{C}_{38}\text{H}_{90}\text{FeKN}_2\text{O}_6\text{Si}_6$ (%): C 48.84 , H 9.71 , N, 3.00 ; found (%): C 48.80 , H 9.39 , N 2.96 %.

Magnetic susceptibility measurements were performed using a Quantum Design MPMS-XL SQUID magnetometer. A detailed description of the sample preparation for the magnetic studies is included in the Supplementary Methods. The a.c. magnetic susceptibility data measurements were performed using a 4 Oe switching field. All data were corrected for diamagnetic contributions from the eicosane restraint and core diamagnetism estimated using Pascal's constants. The a.c. magnetic relaxation data were fitted using formulae that describe χ' and χ'' in terms of frequency, constant temperature susceptibility (χ_T), adiabatic susceptibility (χ_S), relaxation time (τ) and a variable that represents the distribution of relaxation times (α)^{3,47}. The Mössbauer spectra were measured at 5 and 295 K on a constant acceleration spectrometer that utilized a room-temperature ^{57}Co in rhodium source and was calibrated at 295 K with α -iron foil.

Further characterization, computational and crystallographic details for compound **1** are described in the Supplementary Methods. Crystallographic data were collected using a Bruker QUAZAR diffractometer and are deposited in the Cambridge Structural Database as CCDC 908721 (1).

Received 14 November 2012; accepted 18 March 2013;
published online 5 May 2013

References

- Ishikawa, N., Sugita, M., Ishikawa, T., Koshihara, S.-Y. & Kaizu, Y. Lanthanide double-decker complexes functioning as magnets at the single-molecule level. *J. Am. Chem. Soc.* **125**, 8694–8695 (2003).
- Rinehart, J. D. & Long, J. R. Exploiting single-ion anisotropy in the design of *f*-element single-molecule magnets. *Chem. Sci.* **2**, 2078–2085 (2011).
- Gatteschi, D., Sessoli, R. & Villain, J. *Molecular Nanomagnets* (Oxford Univ. Press, 2006).
- Branzoli, F. *et al.* Spin dynamics in the negatively charge terbium(III) bis-phthalocyaninato complex. *J. Am. Chem. Soc.* **131**, 4387–4396 (2009).
- Jiang, S.-D., Wang, B.-W., Sun, H.-L., Wang, Z.-M. & Gao, S. An organometallic single-ion magnet. *J. Am. Chem. Soc.* **133**, 4730–4733 (2011).
- Gonidec, M. *et al.* Surface supramolecular organization of a terbium(III) double-decker complex on graphite and its single molecule magnet behavior. *J. Am. Chem. Soc.* **133**, 6603–6612 (2011).
- Sessoli, R. *et al.* High-spin molecules: $[\text{Mn}_{12}\text{O}_{12}(\text{O}_2\text{CR})_{16}(\text{H}_2\text{O})_4]$. *J. Am. Chem. Soc.* **115**, 1804–1816 (1993).
- Sessoli, R., Gatteschi, D., Caneschi, A. & Novak, M. A. Magnetic bistability in a metal-ion cluster. *Nature* **365**, 141–143 (1993).
- Milios, C. J. *et al.* A record anisotropy barrier for a single-molecule magnet. *J. Am. Chem. Soc.* **129**, 2754–2755 (2007).
- Yoshihara, D., Karasawa, S. & Koga, N. Cyclic single-molecule magnet in heterospin system. *J. Am. Chem. Soc.* **130**, 10460–10461 (2008).
- Mannini, M. *et al.* Magnetic memory of a single-molecule quantum magnet wired to a gold surface. *Nature Mater.* **8**, 194–197 (2009).
- Leuenberger, M. N. & Loss, D. Quantum computing in molecular magnets. *Nature* **410**, 789–793 (2001).
- Ardavan, A. *et al.* Will spin-relaxation times in molecular magnets permit quantum information processing? *Phys. Rev. Lett.* **98**, 057201-1–057201-4 (2007).
- Stamp, P. C. E. & Gaita-Ariño, A. Spin-based quantum computers made by chemistry: hows and whys. *J. Mater. Chem.* **19**, 1718–1730 (2009).
- Bogani, L. & Wernsdorfer, W. Molecular spintronics using single-molecule magnets. *Nature Mater.* **7**, 179–186 (2008).
- Atanasov, M. *et al.* Detailed *ab initio* first-principles study of the magnetic anisotropy in a family of trigonal pyramidal iron(II) pyrrolide complexes. *Inorg. Chem.* **50**, 7460–7477 (2011).
- Freedman, D. E. *et al.* Slow magnetic relaxation in a high-spin iron(II) complex. *J. Am. Chem. Soc.* **132**, 1224–1225 (2010).
- Harman, W. H. *et al.* Slow magnetic relaxation in a family of trigonal pyramidal iron(II) pyrrolide complexes. *J. Am. Chem. Soc.* **132**, 18115–18126 (2010).
- Weismann, D. *et al.* High-spin cyclopentadienyl complexes: a single-molecule magnet based on the aryl-iron(II) cyclopentadienyl type. *Chem. Eur. J.* **17**, 4700–4704 (2011).
- Lin, P.-H. *et al.* Importance of out-of-state spin-orbit coupling for slow magnetic relaxation in mononuclear Fe^{II} complexes. *J. Am. Chem. Soc.* **133**, 15806–15809 (2011).
- Jurca, T. *et al.* Single-molecule magnet behavior with a single metal center enhanced through peripheral ligand modifications. *J. Am. Chem. Soc.* **133**, 15814–15817 (2011).
- Vallejo, J. *et al.* Field-induced slow magnetic relaxation in a six-coordinate mononuclear cobalt(II) complex with a positive anisotropy. *J. Am. Chem. Soc.* **134**, 15704–15707 (2012).
- Kramers, H. A. A general theory of paramagnetic rotation in crystals. *Proc. R. Acad. Sci. Amsterdam* **33**, 959–972 (1930).
- Zadrozny, J. M. & Long, J. R. Slow magnetic relaxation at zero field in the tetrahedral complex $[\text{Co}(\text{SPh})_4]^{2-}$. *J. Am. Chem. Soc.* **133**, 20732–20734 (2011).
- Mossin, S. *et al.* A mononuclear $\text{Fe}(\text{III})$ single molecule magnet with a $3/2 \leftrightarrow 5/2$ spin crossover. *J. Am. Chem. Soc.* **134**, 13651–13661 (2012).
- Power, P. P. Stable two-coordinate, open-shell (d^1 – d^9) transition metal complexes. *Chem. Rev.* **112**, 3482–3507 (2012).
- Reiff, W. M., LaPointe, A. M. & Witten, E. H. Virtual free ion magnetism and the absence of Jahn–Teller distortion in a linear two-coordinate complex of high-spin iron(II). *J. Am. Chem. Soc.* **126**, 10206–10207 (2004).
- Reiff, W. M. *et al.* Consequences of a linear two-coordinate geometry for the orbital magnetism and Jahn–Teller distortion behavior of the high spin iron(II) complex $\text{Fe}[\text{N}(t\text{-Bu})_2]_2$. *J. Am. Chem. Soc.* **131**, 404–405 (2009).
- Merrill, W. A. *et al.* Direct spectroscopic observation of large quenching of first-order orbital angular momentum with bending in monomeric, two-coordinate $\text{Fe}(\text{II})$ primary amido complexes and the profound magnetic effects of the absence of Jahn– and Renner–Teller distortions in rigorously linear coordination. *J. Am. Chem. Soc.* **131**, 12695–12702 (2009).
- Zadrozny, J. M. *et al.* Slow magnetization dynamics in a series of two-coordinate iron(II) complexes. *Chem. Sci.* **4**, 125–138 (2013).
- Atanasov, M. A., Zadrozny, J. M., Long, J. R. & Neese, F. A theoretical analysis of chemical bonding, vibronic coupling, and magnetic anisotropy in linear iron(II) complexes with single-molecule magnet behavior. *Chem. Sci.* **4**, 139–156 (2013).
- Eaborn, C., Hitchcock, P. B., Smith, J. D. & Sullivan, A. C. Crystal structure of the tetrahydrofuran adduct of tris(trimethylsilyl)-methyl-lithium, $[\text{Li}(\text{thf})_4][\text{Li}\{\text{C}(\text{SiMe}_3)_3\}_2]$. *J. Chem. Soc. Chem. Commun.* 827–828 (1983).
- Eaborn, C., Hitchcock, P. B., Smith, J. D. & Sullivan, A. C. Preparation and crystal structure of the tetrahydrofuran adduct of lithium bis[tris(trimethylsilyl)methyl]cuprate, $[\text{Li}(\text{THF})_4][\text{Cu}\{\text{C}(\text{SiMe}_3)_3\}_2]$. The first structural characterization of a Gilman reagent. *J. Organomet. Chem.* **263**, C23–C25 (1984).
- Eaborn, C., Hitchcock, P. B., Smith, J. D. & Sullivan, A. C. Preparation and crystal structure of the argentate complex $[\text{Li}(\text{tetrahydrofuran})_4][\text{Ag}\{\text{C}(\text{SiMe}_3)_3\}_2]$. *J. Chem. Soc. Chem. Commun.* 870–871 (1984).
- Al-Juaid, S. S. *et al.* Metalation of tris(trimethylsilyl)- and tris(dimethylphenylsilyl)methane with methylsodium: the first dialkylsodiate. *Angew. Chem. Int. Ed. Engl.* **33**, 1268–1270 (1994).
- LaPointe, A. M. $\text{Fe}[\text{C}(\text{SiMe}_3)_3]_2$: synthesis and reactivity of a monomeric homoleptic iron(II) alkyl complex. *Inorg. Chim. Acta* **345**, 359–362 (2003).
- Stoian, S. A. *et al.* Mössbauer, electron paramagnetic resonance, and crystallographic characterization of a high-spin $\text{Fe}(\text{I})$ diketiminate complex with orbital degeneracy. *Inorg. Chem.* **44**, 4915–4922 (2005).
- Yu, Y. *et al.* The reactivity patterns of low-coordinate iron-hydride complexes. *J. Am. Chem. Soc.* **130**, 6624–6638 (2008).
- Nakajima, Y. *et al.* Electronic structure of four-coordinate iron(I) complex supported by a bis(phosphaethenyl)pyridine ligand. *J. Am. Chem. Soc.* **132**, 9934–9936 (2010).
- Carlin, R. *Magnetochemistry* (Springer, 1986).
- Gatteschi, D. & Sessoli, R. Quantum tunneling of magnetization and related phenomena in molecular materials. *Angew. Chem. Int. Ed.* **42**, 268–297 (2003).
- Luis, F. *et al.* Spin-lattice relaxation via quantum tunneling in an Er^{3+} -polyoxometalate molecular magnet. *Phys. Rev. B* **82**, 060403(R) (2010).
- Meihaus, K. R., Rinehart, J. D. & Long, J. R. Dilution-induced slow magnetic relaxation and anomalous hysteresis in trigonal prismatic dysprosium(III) and uranium(III) complexes. *Inorg. Chem.* **50**, 8484–8489 (2011).
- Rinehart, J. D. & Long, J. R. Slow magnetic relaxation in homoleptic trispyrazolylborate complexes of neodymium(III) and uranium(III). *Dalton Trans.* **41**, 13572–13574 (2012).
- Rinehart, J. D., Fang, M., Evans, W. & Long, J. R. Strong exchange and magnetic blocking in N_2^{3-} radical-bridged lanthanide complexes. *Nature Chem.* **3**, 538–542 (2011).
- Demir, S., Zadrozny, J. M., Nippe, M. & Long, J. R. Exchange coupling and magnetic blocking in bipyrimidyl radical-bridged lanthanide complexes. *J. Am. Chem. Soc.* **134**, 18546–18549 (2012).
- Cole, K. S. & Cole, R. H. Dispersion and absorption in dielectrics. I. Alternating current characteristics. *J. Chem. Phys.* **9**, 341–351 (1941).

Acknowledgements

This research was funded by the National Science Foundation through grant CHE-1010002. We thank R. Nichiporuk for assistance with ESI/MS acquisition, T. Chantarojsiri, M. Nippe and S. Demir for experimental assistance and M. Fasulo for valuable discussions.

Author contributions

J.M.Z., D.J.X. and J.R.L. planned and executed the synthesis, characterization and magnetic measurements, and analysed the resulting data. M.A. and F.N. performed calculations and analysed the resulting data. G.J.L. and F.G. analysed the Mössbauer spectra. All authors were involved in writing the manuscript.

Additional information

Supplementary information and chemical compound information are available in the online version of the paper. Reprints and permissions information is available online at www.nature.com/reprints. Correspondence and requests for materials should be addressed to J.R.L.

Competing financial interests

The authors declare no competing financial interests.